



1. Introduction

Ever since Richard P. Feynman's keynote speech at the first conference on physics and computation at the MIT in 1981, where he presented his idea of a quantum computer as a simulator of quantum mechanical systems [16], computer scientists and physicists alike expended huge efforts to actually realise such a device. The simulation of quantum mechanical systems by means of other, controllable quantum systems has shown first promising results in recent years as the field of quantum optics has grown to a point where one-, two-, and three-dimensional optical lattices can be constructed by interference of laser light. In these optical lattices, ultracold atomic gases could then be efficiently controlled to simulate solid states of matter. There, e. g. the paramount model of solid state theoretical physics, the Hubbard model, has been shown to be realizable in case of bosonic particles [21].

While the prospect of a quantum simulator is fascinating and desirable to actually probe the models that physicists claim to describe nature, a second branch has emerged that is interested in quantum systems to perform calculations which are not possible on a classical computer.

As the algorithms needed for such a quantum computer are entirely different from classical computer algorithms, only a handful have been devised so far which are known to outperform any classical algorithm. The most prominent ones are those of quantum Fourier transform and its application to the factorisation of large integer numbers and the quantum search, or Grover's algorithm, useful e. g. in the solution of the travelling salesman problem [36].

However, it is not only algorithms that need to be invented in the field of quantum computation but also means to build quantum mechanical systems and control them with high accuracy. Like the NAND logic gate is the universal gate of classical computer, making it possible to build any other logic gate from a number of NAND gates, "any multiple qubit logic gate may be composed from CNOT and single qubit gates" [36], making those the universal building blocks of a quantum computer.

Since at first no physicist had the knowledge of how to build single quantum bits and perform controlled operations on them, a wide field of possible systems have been proposed and built, culminating only recently in the 2012 Physics Nobel prize for Serge Haroche and David J. Wineland "for ground-breaking experimental methods that enable measuring and manipulation of individual quantum systems" [38].

To the author the most promising candidates for scalable arrays of quantum bits, out of which quantum registers may be composed, are quantum dots already realised in GaAs semiconductor devices [43] and recently also in silicon-based semiconductors [17], circuit-quantum electro dynamics (QED) [49, 15] and the aforementioned optical lattice systems with ultra cold atomic gases [29]. Besides these, there is the rather new class of topological insulators where stable topological excitations (particles) may e. g. arise in between the surfaces of topological insulator/superconductor heterostructures [34]. Those topological excitations may then be stable against decoherence, like the

two Majorana-Fermions at the ends of a superconducting nano-wire that have been proposed and arguably been measured [35].

While multiple qubits in a quantum register should behave independently, their connection to the same environment may spoil that independence, as they start to influence each other via the environment. In this work two qubits, modelled by magnetic spin-1/2 impurities, are investigated that are coupled at a finite distance to the same dissipative environment. From the spin-boson model it is known that there exists a phase for weak coupling where the spin is not localised in either of its states $|\uparrow\rangle$ or $|\downarrow\rangle$ and may thus explore the whole $SU(2)$ Bloch sphere, while for strong coupling it is localised in one of those configurations, completely destroying its quantum mechanical nature [27]. As a second spin is coupled in direct vicinity of the first, the environment mediates an effective ferromagnetic interaction between the spins, rendering them no longer independent [41].

Within the Numerical Renormalization Group (NRG) it is investigated at which point the two spins can be treated independently as the distance between them is increased. To this end a two-channel bosonic NRG is developed that can deal with the model and its limit of two independent spin-boson models. The two-channel NRG is first tested on a model incorporating a single oscillator as an impurity. While the latter model only involves a single channel, a self-interaction of the impurity oscillator provides accessible limits, where the numerical implementation of the two-channel NRG can be tested. Furthermore signals of the different impurities are traced in the environment by means of thermal averages and their changes due to the presence of the impurities.

Outline

The thesis presented here is structured as follows. The two dissipative quantum impurity models under discussion, named the dissipative oscillator model (do) and the two-spin-boson model (2sbm) are introduced in detail in section 2. For the environment, a one-dimensional chain of bosons in real space is chosen to which the different impurities are then connected. While the one-dimensional character of the environment allows for a convenient calculation of distance-dependent averages, it is not the generic kind of system to show an ohmic spectrum of excitations, as studied here. The latter is only achieved in this thesis by tuning the particle dispersion and thus in real space the hopping amplitudes of excitations between the different sites in the chain. For the chosen dispersion, however, long range hopping amplitudes that drop in a power-law manner emerge in real-space. To which extent such a dispersion can be achieved in, e.g. optical lattice experiments with very shallow potentials, remains elusive at this point in time. In higher dimensional systems an ohmic spectrum is more likely to appear without the need of such long-range hopping. There the calculation of the distance-dependent averages—of interest in this thesis—turns out to be more complicated to obtain numerically.

Section 3 introduces the concept of correlation functions and illustrates how they may be obtained from a set of equations of motion. Afterwards, the representation of correlation functions in terms of Lehmann-sums and their connection to spectral functions via their imaginary part are stated. The connection between thermal expectation values for the site occupation as well as the average displacement of the environmental oscillators to corresponding correlation functions is drawn in sections 3.4 and 3.5 respectively. The processes that need to be averaged involve both free propagation between different sites and scattering at either one of the impurities.

The scattering processes are encoded in so-called scattering matrices which are purely described in terms of impurity correlation functions. In case of the dissipative oscillator model the scattering matrix is a complex function whereas for the two-spin-boson model it obtains a more complex, 2×2 matrix structure of complex functions. Both the free bath correlators for different distances and the scattering matrices entering the thermal average processes are derived in section 4. Here, it is also shown how the bath spectral functions which enter the different models are connected to the dispersion relation of the bosonic particles in the chain and how the long-range, real-space hopping amplitudes emerge.

Section 5 focuses on the discussion of the Numerical Renormalization Group (NRG) and its application to both models. After its introduction a discussion of how spectral functions can be obtained from the numerical data provided by the NRG follows. Section 5.5 examines the actual implementation of the NRG employing sparse matrix storage formats and Lanczos diagonalisation routines for the appearing Hamiltonians. The computational demands of the current NRG implementation are compared to an implementation which uses dense matrix representations and exact diagonalisation routines as is typical for a single channel NRG.

The results obtained for the two models under discussion are presented in section 6. In both models the renormalization group flow and the fixed point structure of the Hamiltonians that are set up within the NRG are discussed.

Section 6.1 presents the results that have been derived for the dissipative oscillator model. For every value of the self-interaction of the impurity oscillator, the NRG data suggest a quantum phase transition in the dissipative oscillator model as a function of the coupling strength between impurity and environment. In the scattering matrix the pole at the bare oscillator frequency is found to be shifted to lower frequencies as the coupling strength to the environment increases. At the same time, the peak is broadened and its height increased until it finally vanishes beyond the quantum critical point. With the results for the scattering matrix, finally the thermal averages in the environment are calculated as a function of distance to the impurity oscillator. Both the average site occupation and the average displacement of the oscillators are found to change strongest right at the impurity. Going away from the impurity those changes then drop in a power-law manner for a large range of parameters.

For the two-spin-boson model the results are collected in section 6.2. There the fixed point spectra for finite inter-impurity distance are compared to those for zero



distance between the impurities. A localised and a delocalised phase are found to exist for every distance investigated in this work. In the spectrum of the scattering matrix a low energy peak appears that can be assigned to a renormalized tunnelling rate on the impurities. This peak is suppressed as the localised phase is entered and the impurities are each locked in a single configuration. The distance dependent averages that are calculated in the environment show clear peaks right at the position of the two impurities. In between the impurities, it is possible to see their influence on each other by a comparably large finite effect on the environmental oscillators. Far away from the two impurities, the changes they cause in the environment drop in a power-law manner.

As the different techniques used in this thesis are close to identical for the two models under discussion their application to both models is presented consecutively. This is to emphasise similarities and differences between the two models. In each section, the method at hand is first applied to the dissipative oscillator model, followed by an application of the technique to the two-spin-boson model.



2. Introduction of the models

It is the purpose of this work to study the extent to which different quantum impurity systems, coupled to a common dissipative environment, may influence each other via that environment. Both the low-energy physics of the impurities and different thermal averages in the environment will be determined. Thereby it can be estimated to what extent the impurities effectively influence the environment and thus may also influence each other.

For the quantum impurity systems an oscillator of bosonic nature and two spin-1/2 particles that are coupled at a finite distance R to a common environment are chosen. The dissipative environment itself is modelled in real-space by a one-dimensional chain of bosonic orbitals. The signals that are investigated in the environment are the change of the average site occupation $\Delta\langle\hat{n}_x\rangle$ and the change of the average of the squared displacement $\Delta\langle(a_x + a_x^\dagger)^2\rangle$ of the oscillators at position x in the chain due to the coupling of the impurities to the chain. In the following the two different models under investigation in this work are introduced, which are both connected to the renowned spin-boson model, already investigated by Leggett et al. in 1987 [27]. In that case, a two-state system is coupled to a dissipative environment and the setup is such that the bare two-state system may tunnel between its two states with a rate Δ . As the coupling to the environment is increased the tunnelling rate is suppressed until it eventually becomes zero, freezing the spin in either of its two possible configurations and thereby destroying its quantum mechanical nature.

The otherwise harmonic oscillator in the dissipative oscillator model discussed here features a self-interaction which, as it is increased, projects out higher lying states of the impurity until only two states are left that can be identified with a spin-1/2 system. In case of the two spins of the second model they become independent in the limit of infinite distance R between them and thus each behave as the single spin-1/2 in the spin-boson model.

2.1. Dissipative oscillator model

The first model under investigation features an oscillator with frequency Δ that is subject to dissipation introduced by an environment. The single oscillator here and in the following is termed the impurity as it has in general a different character from the oscillators of the environment. Its Hamiltonian is given by

$$H_{\text{imp}} = \Delta\left(\hat{n}_b + \frac{1}{2}\right) + \epsilon\left(\frac{b + b^\dagger}{2}\right) + \frac{U}{2}\hat{n}_b(\hat{n}_b - 1) \quad (2.1)$$

where b^\dagger creates an excitation of the oscillator that features, apart The underlying potential in real-space is still quadratic, rendering the oscillator harmonic. However, the self-interaction via its density makes coherent states of the harmonic oscillator, which are the next best thing to a classical particle moving in a square potential well,

decohere in time as the eigenenergies of the different states $|n\rangle$ are no longer multiples of the bare oscillator frequency Δ . The environment of the impurity is modelled by an infinite chain of bosons. In real space the bosonic operator $a_{x_i}^\dagger$ creates a particle at position $x_i = ia$ in the chain. Here a is the lattice spacing and $i \in \mathbb{Z}$. The particle can hop with an amplitude $t_{x_i, x_j} = t_{|x_i - x_j|}$ between any two sites x_i and x_j . Typically hopping amplitudes fall off with growing distance $|x_{ij}| = |x_i - x_j|$. In this model the hopping amplitudes are considered to be real and the lattice spacing a to unity are set in the following. Thus the Hamiltonian describing the translational invariant environment can be written as

$$H_{\text{bath}} = \sum_{i, j \in \mathbb{Z}} t_{|x_i - x_j|} a_{x_i}^\dagger a_{x_j} = \sum_{x, y \in \mathbb{Z}} t_{|x|} a_y^\dagger a_{y-x}. \quad (2.2)$$

Dissipation is introduced into the model by coupling the displacement of the impurity to the displacement of the bosonic degree of freedom at the origin of the bath. The interaction part of the model is then given by

$$H_{\text{int}} = \frac{\sqrt{\alpha}}{2} (b + b^\dagger) (a_0 + a_0^\dagger). \quad (2.3)$$

Here α parametrises the coupling strength between the impurity and the bath. Thus the total Hamiltonian of the dissipative oscillator model is given by

$$H_{\text{do}} = H_{\text{imp}} + H_{\text{bath}} + H_{\text{int}},$$

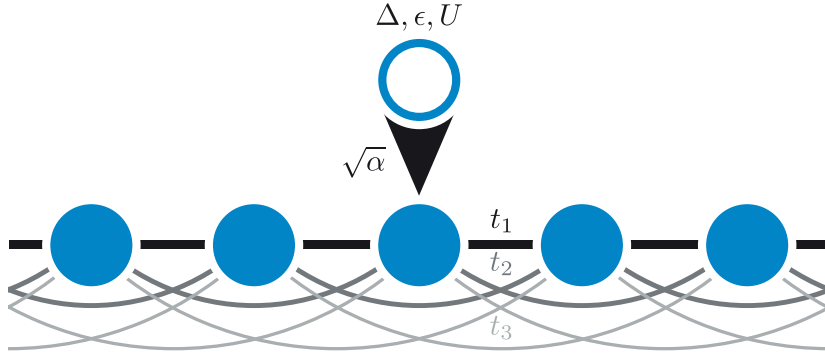
where H_{imp} describes the oscillator of interest (the impurity), H_{bath} describes the free environment and H_{int} comprises the interaction between the oscillator and the bath as mentioned above.

In figure 1, a sketch of the system around the origin is shown which comprises all relevant energy-scales. In order to diagonalise the bath part of the Hamiltonian a Fourier-transformation of the lattice is performed via

$$a_k = \frac{1}{\sqrt{2\pi}} \sum_{x \in \mathbb{Z}} a_x e^{ikx}, \quad a_x = \frac{1}{\sqrt{2\pi}} \int_{-\pi}^{\pi} a_k e^{-ikx} dk. \quad (2.4)$$

Here the integral in k -space is over the first Brillouin-zone. Applying the Fourier-transformation to the bath part of the Hamiltonian leads to

$$\begin{aligned} H_{\text{bath}} &= \frac{1}{2\pi} \sum_{x, y} t_{|x|} \int_{-\pi}^{\pi} \int_{-\pi}^{\pi} a_k^\dagger a_{k'} e^{i(k-k')y} e^{ik'x} dk dk' \\ &= \sum_x t_{|x|} \int_{-\pi}^{\pi} \int_{-\pi}^{\pi} a_k^\dagger a_{k'} \delta(k - k') e^{ik'x} dk dk' \\ &= \int_{-\pi}^{\pi} a_k^\dagger a_k \sum_x t_{|x|} e^{ikx} dk \\ &= \int_{-\pi}^{\pi} \omega(k) a_k^\dagger a_k dk \end{aligned}$$


Figure 1:

The impurity (circle) with energy-scales Δ, ϵ, U couples with a strength $\sqrt{\alpha}$ to the origin of a linear chain of bosons (disks). The bosons in the chain can hop between any two sites where the hopping amplitudes t_x decrease with the distance x between the sites in a power-law manner. Here, only the first three hopping amplitudes t_1, t_2 and t_3 are depicted for clarity.

where $\omega(k) = \sum_x t_{|x|} e^{ikx}$ is the dispersion of the bath-modes. The interaction part of the model is likewise transformed to

$$H_{\text{int}} = \frac{1}{2} \sqrt{\frac{\alpha}{2\pi}} (b + b^\dagger) \int_{-\pi}^{\pi} (a_k + a_k^\dagger) dk.$$

The total Hamiltonian describing the oscillator with bare frequency Δ which can be damped by the coupling to a one dimensional chain of bosons thus reads

$$H_{\text{do}} = H_{\text{imp}} + \int_{-\pi}^{\pi} \omega(k) a_k^\dagger a_k dk + \frac{1}{2} \sqrt{\frac{\alpha}{2\pi}} (b + b^\dagger) \int_{-\pi}^{\pi} (a_k + a_k^\dagger) dk \quad (2.5)$$

in momentum space.

Until now there were not any specific hopping parameters $t_{|x|}$ chosen, they were merely considered to be real and expected to drop with growing distance. The $t_{|x|}$ are connected to the spectral function of the bath via the dispersion relation $\omega(k)$. In this work, models which show a power-law behaviour in the spectral function of the chain are investigated. The spectral function here is parametrised as

$$J(\omega) = \begin{cases} \alpha\pi(s+1)\omega^s\omega_c^{1-s} & , \text{ for } 0 \leq \omega \leq \omega_c \\ 0 & , \text{ else.} \end{cases} \quad (2.6)$$

Here $s > -1$ is the power-law exponent, α parametrises the coupling strength between bath and impurity and ω_c is a high-frequency cutoff. Throughout this thesis only models that show an ohmic spectral density where $s = 1$ are investigated. In section

4.1 it will be discussed that the spectral function $J(\omega)$ is connected to the imaginary part of the local retarded Green's function $\langle\langle a_0, a_0^\dagger \rangle\rangle_{\omega+i\epsilon}$ at the origin of the bath in real space as

$$\begin{aligned} J(\omega) &= -\alpha \lim_{\epsilon \rightarrow 0} \text{Im}[\langle\langle a_0, a_0^\dagger \rangle\rangle_{\omega+i\epsilon}] \\ &= \frac{\alpha}{2} \int_{-\pi}^{\pi} \delta(\omega - \omega(k)) dk. \end{aligned} \quad (2.7)$$

In the spectral function $J(\omega)$ all information on the single-particle-excitations of the non-interacting bath, which couples to the impurity, is comprised. Besides it will be shown in section 4.1 how one has to adjust the dispersion $\omega(k)$ in order to arrive at the desired behaviour (2.6) of the spectral function. Furthermore it will be validated that the corresponding hopping amplitudes $t_{|x|}$ do drop in a power-law manner in real space as $t_{|x|} \sim |x|^{-(s+2)/(s+1)}$. For the later treatment of the model by means of the Numerical Renormalization Group (NRG) the Hamiltonian is presented here directly in frequency space, which is the usual representation to start with in the NRG-community. Expressing the bath excitations directly in terms of their corresponding frequencies ω instead of their momenta k , the Hamiltonian of the dissipative oscillator model can be rewritten as

$$H = H_{\text{imp}} + \int_0^{\omega_c} g(\omega) a_\omega^\dagger a_\omega d\omega + \frac{1}{2} (b + b^\dagger) \int_0^{\omega_c} h(\omega) (a_\omega + a_\omega^\dagger) d\omega. \quad (2.8)$$

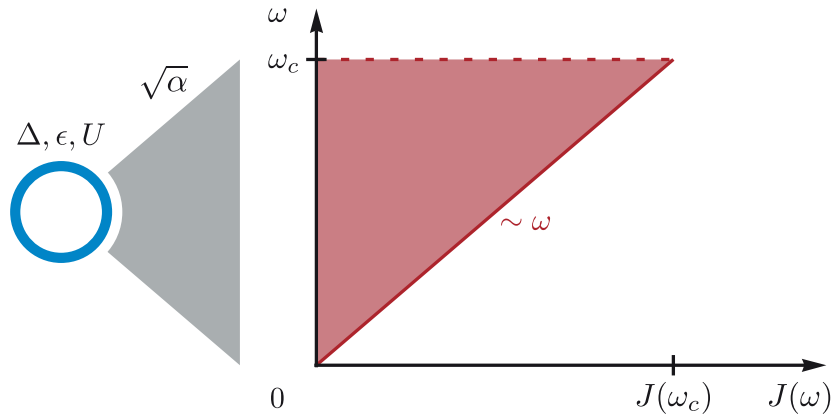
Here the function $g(\omega)$ comprises the possible excitations of the bath modes at frequency ω and the function $h(\omega)$ encodes the coupling of the impurity to those excitations. The functions $g(\omega)$ and $h(\omega)$ are connected to the spectral function $J(\omega)$ [12] by:

$$J(\omega) = \pi \left| \frac{\partial g(\omega)}{\partial \omega} \right|^{-1} h^2(\omega). \quad (2.9)$$

Figure 2 depicts the situation where the impurity couples to a continuous bath that is described by its spectral function $J(\omega)$ given by (2.6) for an ohmic environment with $s = 1$. As the high-frequency cutoff ω_c should represent the largest energy-scale in the problem, all other parameters in the model will be given in units of that cutoff. This way ω_c is factored out leaving the dimensionless Hamiltonian

$$\boxed{\frac{H_{\text{do}}}{\omega_c} = H_{\text{imp}} \left(\frac{\Delta}{\omega_c}, \frac{\epsilon}{\omega_c}, \frac{U}{\omega_c} \right) + \int_0^1 g(\omega) a_\omega^\dagger a_\omega d\omega + \frac{1}{2} (b + b^\dagger) \int_0^1 h(\omega) (a_\omega + a_\omega^\dagger) d\omega.} \quad (2.10)$$

For fixed power-law exponent s and high frequency cutoff ω_c , the model possesses four remaining parameters: the bare frequency of the impurity oscillator Δ , its displacement ϵ , its self-interaction strength U via its local density and finally the coupling strength α of the impurity to the environment. In the following all parameters $X \in \{\Delta, \epsilon, U\}$ are given in units of ω_c and the explicit notation is dropped, keeping only the bare parameter name ($X \hat{=} \frac{X}{\omega_c}$).


Figure 2:

The impurity (circle) with energy-scales Δ, ϵ, U couples with a strength $\sqrt{\alpha}$ to a continuous bath of bosons characterised by the spectral density $J(\omega)$. Here the bath features an ohmic spectral density $J(\omega) \sim \omega$ and corresponds in real-space to the linear chain as depicted in figure 1.

Large- U limit: the spin-boson model

The dissipative oscillator model transforms into the spin-boson model as the on-site interaction U is made stronger and stronger. If the impurity Hamiltonian H_{imp} is expressed in the basis of eigenstates $|n\rangle$ of the number operator $b^\dagger b$, its diagonal elements read

$$\langle n | H_{\text{imp}} | n \rangle = \Delta \left(n + \frac{1}{2} \right) + \frac{U}{2} n(n-1).$$

In the limit of $U \rightarrow \infty$ all states with $n > 1$ are separated from the low energy sector of the theory by an infinite amount of energy and therefore can be effectively projected out. Hence the impurity Hamiltonian is restricted to the two-dimensional basis $\{|0\rangle \hat{=} |\uparrow\rangle, |1\rangle \hat{=} |\downarrow\rangle\}$ where it reads

$$\lim_{U \rightarrow \infty} H_{\text{imp}} = \frac{1}{2} \begin{pmatrix} -\Delta & \epsilon \\ \epsilon & \Delta \end{pmatrix} = \frac{\epsilon}{2} \sigma_x - \frac{\Delta}{2} \sigma_z$$

after the ground-state-energy is shifted by an amount of $-\Delta$. Likewise the interaction part H_{int} is transformed to

$$H_{\text{int}} = \sqrt{\frac{\alpha}{2\pi}} \frac{\sigma_x}{2} \int_{-\pi}^{\pi} (a_k + a_k^\dagger) dk.$$

Thus the total Hamiltonian reads

$$H_{\text{sbm}} = \frac{\epsilon}{2} \sigma_x + \frac{\Delta}{2} \sigma_z + \int_{-\pi}^{\pi} \omega(k) a_k^\dagger a_k dk + \sqrt{\frac{\alpha}{2\pi}} \frac{\sigma_x}{2} \int_{-\pi}^{\pi} (a_k + a_k^\dagger) dk. \quad (2.11)$$

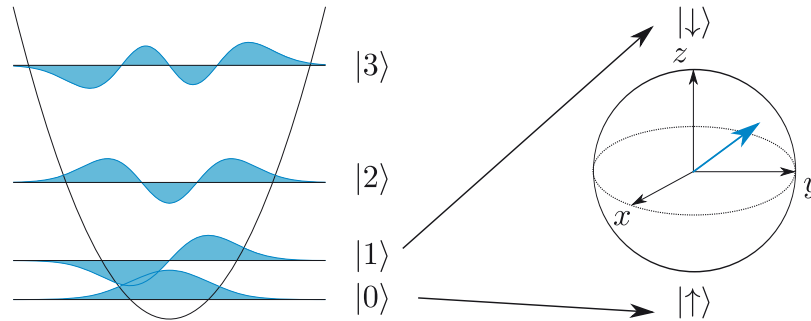


Figure 3:

As the density-density interaction U is increased, all states but the lowest two $|0\rangle$ and $|1\rangle$ of the oscillator are projected out. Those can then be mapped onto a spin-degree of freedom living on the $SU(2)$ sphere.

which is the Hamiltonian of the well studied spin-boson model [27] in momentum representation. Figure 3 depicts the situation where the higher lying oscillator states $|n\rangle$ with $n > 1$ are shifted due to the interaction U . In the end only the two lowest states remain in the theory which then can be mapped onto a spin-1/2 degree of freedom living on the $SU(2)$ sphere. It will be shown numerically in section 6.1.3 that the low energy spectrum of the spin-boson model and the displaced oscillator model agree already for values of $U \sim 10^3$.

In the simplest case of a magnetic field of strength Δ only applied in x -direction and no coupling to the environment, measuring the chance that the spin has returned to an initial state $|\sigma(0)\rangle = |\uparrow\rangle$ after time t leads to the perfect periodic result $\langle \uparrow | \sigma(t) \rangle = \cos(\Delta t/2)$. As the coupling to the environment in z -direction is switched on two things will happen. First of all the oscillations get damped as the environment leads to dissipation. Second of all the frequency Δ of the spin oscillations is decreased as the spin becomes somewhat dressed by environmental fluctuations and is no longer free. Ultimately, strong coupling of the environment to the spin will pin it in a single state for which then $\langle \uparrow | \sigma(t) \rangle = \text{const}$ follows and the quantum mechanical nature of the spin has been destroyed.

2.2. Two-spin-boson model

The second model investigated in this work is termed the two-spin-boson model. It describes two spin-1/2 particles that couple to a common dissipative environment. Here the environment is again modelled by the one-dimensional chain of bosons introduced in the dissipative oscillator model (cf. equation (2.2)). Each of the two spins now couples to a lattice site $\pm r$ with a total of $R = 2r$ environmental lattice sites in between them where $r = 0, 1/2, 1, 3/2, \dots$. Of interest in this study is the behaviour of the two spins as the distance R between them is increased. The Hamiltonian of the model has again the general form